PAPER

Joint Transmit/Receive MMSE-FDE for Analog Network Coded Single-Carrier Bi-directional Multi-Antenna Relay

Hiroyuki MIYAZAKI[†a)], **Tatsunori OBARA**[†], *Student Members*, *and* **Fumiyuki ADACHI**[†], *Fellow*

SUMMARY In this paper, joint transmit/receive frequency-domain equalization (FDE) is proposed for analog network coded (ANC) single-carrier (SC) bi-directional multi-antenna relay. In the proposed scheme, diversity transmission using transmit FDE is performed at relay station (RS) equipped with multiple antennas while receive FDE is carried out at base station (BS) and mobile terminal (MT) both equipped with single antenna. The transmit and receive FDE weights are jointly optimized so as to minimize the end-to-end mean square error (MSE). We evaluate, by computer simulation, the throughput performance and show that the joint transmit/receive FDE obtains the spatial and frequency diversity gains and accordingly achieve better throughput performance compared to either the transmit FDE only or the receive FDE only. It is also shown that ANC SC bi-directional multi-antenna relay can extend the communication coverage area for the given required throughput compared to conventional direct transmission.
key words: *analog network coding, single-carrier transmission, joint transmit/receive frequency-domain equalization*

1. Introduction

Next generation mobile communication systems must support broadband data services. However, the throughput of a user close to the cell edge degrades due to propagation path loss and shadowing loss. The 2 time-slot cooperative relay is a promising solution [1]. 2 time-slot cooperative relay can reduce the impact of the propagation path loss and the shadowing loss. However, it requires 4 time-slots for bi-directional communications. Applying network coding to bi-directional relay communications can reduce the required number of time-slots [2]–[5]. There are two types of network coding: digital network coding (DNC) [2] and analog network coding (ANC) [3]–[5]. DNC is based on the decode-and-forward (DF) relaying protocol and can achieve 4/3 times higher maximum throughput than conventional half duplex relaying. On the other hand, ANC is based on the amplify-and-forward relaying protocol and can achieve 2 times higher maximum throughput than the conventional relaying.

The broadband channel is characterized by frequency-selective fading [6]. Although orthogonal frequency division multiplexing (OFDM) can overcome the frequency-selective fading [7], it has a drawback of high peak-to-average power ratio (PAPR) and hence, high-performance amplifiers need to be used [8]. Single-carrier (SC) transmission with minimum mean square error (MMSE) based FDE [9], [10] has an advantage of lower PAPR than OFDM while exploiting the channel selectivity to improve the throughput. Further throughput improvement is achieved by introducing the joint transmit/receive MMSE-FDE [11]. Also promising is the use of multiple antennas at relay station (RS) [12]–[14]. In [14], the beamforming for bi-directional multi-antenna relay communications was investigated. By employing the beamforming, the spatial diversity gain can be obtained. However, Ref. [14] assumes non-frequency-selective fading and focuses on the capacity bound. Therefore, equalization is not considered in [14]. In addition to multi-antennal relay, an introduction of joint transmit/receive FDE may further improve the throughput performance.

In this paper, we propose a joint transmit/receive MMSE-FDE for ANC SC bi-directional multi-antenna relay. In the proposed scheme, diversity transmission using transmit FDE is performed at RS equipped with multiple antennas while receive FDE is carried out at base station (BS) and mobile terminal (MT) both equipped with single antenna. In ANC relay, RS amplifies and forwards its received noise to both BS and MT. Since the MT-RS and RS-BS link qualities are different, the noise power forwarded from RS is different at BS and MT. As a consequence, the transmit FDE weight which simultaneously minimizes the uplink and downlink MSEs does not exist. Therefore, in this paper, we derive the transmit FDE weights optimized separately for the uplink (MT to BS) and the downlink (BS to MT). Also, we derive the corresponding receive FDE weights to be used at BS and MT. We evaluate, by computer simulation, the throughput performance and show that the joint transmit/receive FDE obtains the spatial and frequency diversity gains and accordingly achieve better throughput performance compared to either the transmit FDE only or the receive FDE only. Furthermore, in this paper, we evaluate the spatial distribution of the throughput and show that ANC SC bi-directional multi-antenna relay using joint transmit/receive FDE can extend the communication coverage compared to conventional direct transmission.

The rest of this paper is organized as follows. Section 2 presents the system model and signal representation for the proposed SC ANC bi-directional multi-antenna relay. Section 3 derives the joint transmit/receive FDE weights. Section 4 discusses the computer simulation results. Section 5 offers some concluding remarks.

Manuscript received January 18, 2013.
Manuscript revised July 29, 2013.
[†]The authors are with the Department of Communications Engineering, Graduate School of Engineering, Tohoku University, Sendai-shi, 980-8579 Japan.
a) E-mail: miyazaki@mobile.ecei.tohoku.ac.jp
DOI: 10.1587/transcom.E96.B.3153

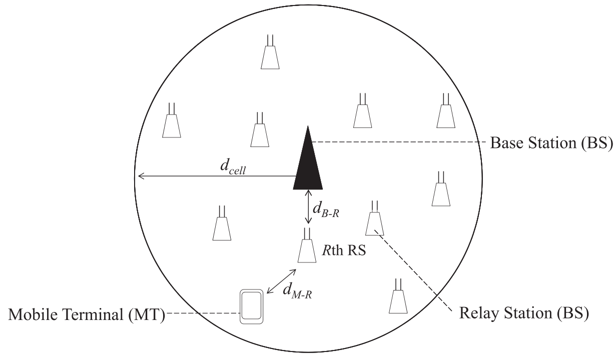

Fig. 1 System model.

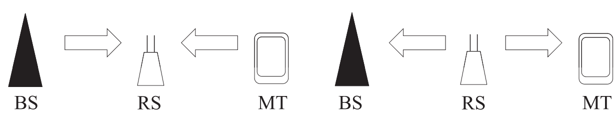

(a) First time-slot (b) Second time-slot

Fig. 2 ANC protocol.

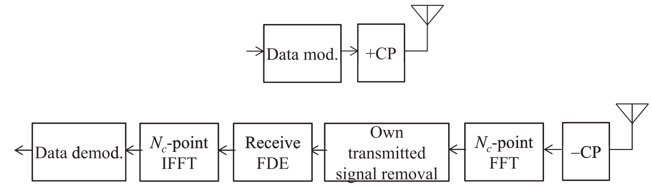

(a) Structure of BS and MT

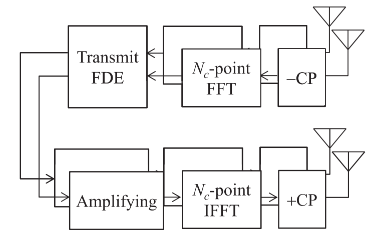

(b) Structure of RS

Fig. 3 Transmitter/receiver structures of MT, BS and RS.

2. System Model and Signal Representation

2.1 System Model

Figure 1 illustrates the system model of bi-directional multi-antenna relay. The single-cell and single-user environment is assumed. The cell radius is denoted by d_{cell}. I RSs are located entire the cell. The distances between MT and RS a nd between BS and RS are respectively denoted by d_{M-R} and d_{B-R}. It is assumed that RS is equipped with J antennas and that BS and MT are equipped with single antenna. The index of RS selected is denoted by $R \in \{0, 1, \ldots, I-1\}$.

2.2 Signal Processing of Multi-Antenna ANC

ANC relay requires two time-slots as seen in Fig. 2. In the first time-slot, RS receives the superposition of two signals transmitted simultaneously from BS and MT. In the second time-slot, RS carries out diversity transmission after transmit FDE to BS and MT. At each of BS and MT, the own transmitted signal is removed from the received signal and receive FDE is carried out.

2.3 Signal Representation

In this paper, symbol-spaced discrete-time signal representation is used. Figure 3 shows the transmitter/receiver structure of MT, RS, and BS.

(a) First time-slot

The data symbol blocks of N_c symbols at BS and MT are denoted as $\{x_B(t): t=0,\ldots,N_c-1\}$ and $\{x_M(t): t=0,\ldots,N_c-1\}$, respectively. After insertion of N_g sample cyclic prefix (CP) into the beginning of each block, BS and MT simultaneously transmit their symbol blocks to RS in the first time-slot. At RS, after CP removal, the received signal is transformed into the frequency-domain signal by N_c-point fast Fourier transform (FFT). The frequency-domain received signal $\{Y_R(j,k): k=0,\ldots,N_c-1, j=0,\ldots,J-1\}$ at jth RS antenna can be expressed as

$$\begin{aligned} Y_R(j,k) &= \sqrt{2\bar{P}_B d_{B-R}^{-\alpha} 10^{-\frac{\eta_{B-R}}{10}}}\,\bar{H}_{B-R}(j,k)X_B(k) \\ &\quad + \sqrt{2\bar{P}_M d_{M-R}^{-\alpha} 10^{-\frac{\eta_{M-R}}{10}}}\,\bar{H}_{M-R}(j,k)X_M(k) + N_R(j,k). \end{aligned} \tag{1}$$

In Eq. (1), $\bar{P}_B$ and $\bar{P}_M$ are the transmit powers of BS and MT, respectively. $\bar{H}_{B-R}(j,k)$ and $\bar{H}_{M-R}(j,k)$ denote the channel transfer functions between BS and jth RS antenna and between MT and jth RS antenna, respectively. α is the propagation path loss exponent. η_{B-R} and η_{M-R} denote the shadowing losses in dB between BS and RS and between MT and RS, respectively. $N_R(j,k)$ is the independent zero-mean complex-valued additive white Gaussian noise (AWGN) having variance $2N_0/T_s$ with N_0 and T_s being the single-sided power spectrum density of AWGN and the symbol duration, respectively. $X_B(k)$ and $X_M(k)$ are the transmit signal components at BS and MT, respectively. They are given as

$$\begin{cases} X_B(k) = \dfrac{1}{\sqrt{N_c}} \displaystyle\sum_{t=0}^{N_c-1} x_B(t) \exp(-j2\pi kt/N_c) \\ X_M(k) = \dfrac{1}{\sqrt{N_c}} \displaystyle\sum_{t=0}^{N_c-1} x_M(t) \exp(-j2\pi kt/N_c) \end{cases}. \tag{2}$$

Equation (1) can be rewritten as

$$\begin{aligned} Y_R(j,k) &= \sqrt{2P_B} H_{B-R}(j,k)X_B(k) \\ &\quad + \sqrt{2P_M} H_{M-R}(j,k)X_M(k) + N_R(j,k) \end{aligned}, \tag{3}$$

where $P_B = \bar{P}_B d_{cell}^{-\alpha}$ and $P_M = \bar{P}_M d_{cell}^{-\alpha}$ are the normalized transmit powers of BS and MT, respectively. $H_{B-R}(j,k)$ and

$H_{M-R}(j,k)$ denote the channel transfer functions, including the impact of the propagation path loss and the shadowing loss, between BS and RS and between MT and RS, respectively. They are given as

$$\begin{cases} H_{B-R}(j,k) = \bar{H}_{B-R}(j,k)\sqrt{r_{B-R}^{-\alpha}10^{-\eta_{B-R}/10}} \\ H_{M-R}(j,k) = \bar{H}_{M-R}(j,k)\sqrt{r_{M-R}^{-\alpha}10^{-\eta_{M-R}/10}} \end{cases}, \tag{4}$$

where $r_{B-R} = d_{B-R}/d_{cell}$ and $r_{M-R} = d_{M-R}/d_{cell}$ are the normalized distances between BS and RS and between MT and RS, respectively.

RS applies FDE to the frequency-domain received signal and amplifies it. The frequency-domain received signal, $\left\{\hat{Y}_R(j,k): k=0,\ldots,N_c-1, j=0,\ldots,J-1\right\}$, after FDE at jth RS antenna can be expressed as

$$\hat{Y}_R(j,k) = G(j)Y_R(j,k)V(j,k), \tag{5}$$

where $V(j,k)$ denotes the transmit FDE weight at jth RS antenna. The transmit FDE weight has a constraint in order to keep the average transmit power of RS constant as

$$\frac{1}{N_c}\sum_{k=0}^{N_c-1}\sum_{j=0}^{J-1}|V(j,k)|^2 = 1. \tag{6}$$

$G(j)$ is the amplifying factor at jth RS antenna. The amplifying factor $G(j)$ is set so as to keep the average transmit power of RS constant as

$$G(j) = \sqrt{\frac{2P_R}{E\left[|Y_R(j,k)|^2\right]}} = \sqrt{\frac{P_R}{\frac{P_M}{N_c}\sum_{k=0}^{N_c-1}|H_{M-R}(j,k)|^2 + \frac{P_B}{N_c}\sum_{k=0}^{N_c-1}|H_{B-R}(j,k)|^2 + N}}, \tag{7}$$

where $P_R = \bar{P}_R d_{cell}^{-\alpha}$ is the normalized transmit power of RS with $\bar{P}_R$ denoting the transmit power of RS and $N = N_0/T_s$ is the noise power.

(b) Second time-slot

The equalized frequency-domain signal is transformed back to time-domain signal by N_c-point inverse FFT (IFFT). After CP insertion, RS broadcasts it to BS and MT in the second time-slot. At BS and MT receiver, after CP removal, the received signals at BS and MT are transformed into the frequency-domain signals. The frequency-domain signals, $\{Y_B(k): k=0,\ldots,N_c-1\}$ and $\{Y_M(k): k=0,\ldots,N_c-1\}$, at BS and MT can be respectively expressed as

$$\begin{cases} Y_B(k) = \sum_{j=0}^{J-1} H_{B-R}(j,k)\hat{Y}_R(j,k) + N_B(k) \\ Y_M(k) = \sum_{j=0}^{J-1} H_{M-R}(j,k)\hat{Y}_R(j,k) + N_M(k) \end{cases}, \tag{8}$$

where $N_B(k)$ and $N_M(k)$ are the zero-mean AWGNs at BS and MT having variance $2N_0/T_s$, respectively. From Eqs. (3) and (5), Eq. (8) can be rewritten as

$$\begin{cases} Y_B(k) = \sqrt{2P_M}\sum_{j=0}^{J-1}G(j)H_{B\text{-}R}(j,k)H_{M\text{-}R}(j,k)V(j,k)X_M(k) \\ \quad +\sqrt{2P_B}\sum_{j=0}^{J-1}G(j)H_{B\text{-}R}(j,k)H_{B\text{-}R}(j,k)V(j,k)X_B(k) \\ \quad +\sum_{j=0}^{J-1}G(j)H_{B\text{-}R}(j,k)V(j,k)N_R(j,k) + N_B(k) \\ Y_M(k) = \sqrt{2P_B}\sum_{j=0}^{J-1}G(j)H_{M\text{-}R}(j,k)H_{B\text{-}R}(j,k)V(j,k)X_B(k) \\ \quad +\sqrt{2P_M}\sum_{j=0}^{J-1}G(j)H_{M\text{-}R}(j,k)H_{M\text{-}R}(j,k)V(j,k)X_M(k) \\ \quad +\sum_{j=0}^{J-1}G(j)H_{M\text{-}R}(j,k)V(j,k)N_R(j,k) + N_M(k) \end{cases}. \tag{9}$$

The first and the second term are the desired signal and the own transmitted signal, respectively. The third term is the noise which is amplified and broadcast by RS. The own transmitted signal is removed from the received signal as

$$\begin{cases} \tilde{Y}_B(k) = Y_B(k) \\ \quad -\sqrt{2P_B}\sum_{j=0}^{J-1}G(j)H_{B\text{-}R}(j,k)H_{B\text{-}R}(j,k)V(j,k)X_B(k) \\ \tilde{Y}_M(k) = Y_M(k) \\ \quad -\sqrt{2P_M}\sum_{j=0}^{J-1}G(j)H_{M\text{-}R}(j,k)H_{M\text{-}R}(j,k)V(j,k)X_M(k) \end{cases}. \tag{10}$$

After the own transmitted signal removal, the receive FDE is carried out. The received signals after receive FDE at BS and MT, $\left\{\hat{Y}_B(k): k=0,\ldots,N_c-1\right\}$ and $\left\{\hat{Y}_M(k): k=0,\ldots,N_c-1\right\}$, can be respectively given as

$$\begin{cases} \hat{Y}_B(k) = \tilde{Y}_B(k)W_B(k) \\ \hat{Y}_M(k) = \tilde{Y}_M(k)W_M(k) \end{cases}, \tag{11}$$

where $W_B(k)$ and $W_M(k)$ are the receive FDE weights at BS and MT receiver, respectively. The equalized signals are transformed back to the time-domain signal by N_c-point IFFT, and the data demodulation is carried out.

3. Joint Transmit/Receive MMSE-FDE

The end-to-end MSEs, e_u and e_d, are respectively defined for the uplink and downlink as

$$\begin{cases} e_u = \sum_{k=0}^{N_c-1} E\left[\left|X_M(k) - \hat{Y}_B(k)\right|^2\right] \\ e_d = \sum_{k=0}^{N_c-1} E\left[\left|X_B(k) - \hat{Y}_M(k)\right|^2\right] \end{cases}. \tag{12}$$

From Eqs. (9), (10) and (11), Eq. (12) can be rewritten as

$$\begin{cases} e_u = \sum_{k=0}^{N_c-1} \left[\begin{array}{l} \left|\sqrt{2P_M}\tilde{H}(k)W_B(k)-1\right|^2 \\ +2N\left\{\sum_{j=0}^{J-1}|G(j)H_{B\text{-}R}(j,k)V(j,k)|^2+1\right\}|W_B(k)|^2 \end{array} \right] \\ e_d = \sum_{k=0}^{N_c-1} \left[\begin{array}{l} \left|\sqrt{2P_B}\tilde{H}(k)W_M(k)-1\right|^2 \\ +2N\left\{\sum_{j=0}^{J-1}|G(j)H_{M\text{-}R}(j,k)V(j,k)|^2+1\right\}|W_M(k)|^2 \end{array} \right] \end{cases}, \tag{13}$$

where

$$\tilde{H}(k) = \sum_{j=0}^{J-1} G(j)H_{B-R}(j,k)H_{M-R}(j,k)V(j,k). \tag{14}$$

From $\partial e_u/\partial W_B(k) = 0$ and $\partial e_d/\partial W_M(k) = 0$, the receive FDE weights at BS and MT are derived as

$$\begin{cases} W_B(k) = \dfrac{\sqrt{2P_M}\tilde{H}^*(k)}{2P_M\left|\tilde{H}(k)\right|^2+2N\left\{\sum_{j=0}^{J-1}|G(j)H_{B-R}(j,k)V(j,k)|^2+1\right\}} \\ W_M(k) = \dfrac{\sqrt{2P_B}\tilde{H}^*(k)}{2P_B\left|\tilde{H}(k)\right|^2+2N\left\{\sum_{j=0}^{J-1}|G(j)H_{M-R}(j,k)V(j,k)|^2+1\right\}} \end{cases}, \tag{15}$$

Substituting Eq. (15) to Eq. (13), we obtain

$$\begin{cases} e_u = \sum_{k=0}^{N_c-1} \dfrac{\left\{\sum_{j=0}^{J-1}|G(j)H_{B-R}(j,k)V(j,k)|^2+1\right\}\left(\frac{P_M}{N}\right)^{-1}}{\left|\tilde{H}(k)\right|^2+\left\{\sum_{j=0}^{J-1}|G(j)H_{B-R}(j,k)V(j,k)|^2+1\right\}\left(\frac{P_M}{N}\right)^{-1}} \\ e_d = \sum_{k=0}^{N_c-1} \dfrac{\left\{\sum_{j=0}^{J-1}|G(j)H_{M-R}(j,k)V(j,k)|^2+1\right\}\left(\frac{P_B}{N}\right)^{-1}}{\left|\tilde{H}(k)\right|^2+\left\{\sum_{j=0}^{J-1}|G(j)H_{M-R}(j,k)V(j,k)|^2+1\right\}\left(\frac{P_B}{N}\right)^{-1}} \end{cases}, \tag{16}$$

Below, we derive joint transmit/receive MMSE-FDE for the uplink and the downlink.

3.1 Uplink Transmit and Receive FDE Weights

The optimization problem for obtaining the uplink transmit FDE weight is expressed as

$$\begin{array}{ll} \text{minimize } e_u & \\ \text{s.t.} & \sum_{k=0}^{N_c-1}\sum_{j=0}^{J-1}|V(j,k)|^2-N_c=0, \\ & |V(j,k)|^2\geq 0,\, j=0,\ldots,J-1,\, k=0,\ldots,N_c-1 \end{array}. \tag{17}$$

By using Caushy-Schwarz inequality [15], e_u is satisfied as

$$e_u \leq \sum_{k=0}^{N_c-1} \frac{\left\{\sum_{j=0}^{J-1}|G(j)H_{B-R}(j,k)V(j,k)|^2+1\right\}\left(\frac{P_M}{N}\right)^{-1}}{\left[\begin{array}{l}\left(\sum_{j=0}^{J-1}|G(j)H_{B-R}(j,k)H_{M-R}(j,k)|^2\right)\left(\sum_{j=0}^{J-1}|V(j,k)|^2\right) \\ +\left\{\sum_{j=0}^{J-1}|G(j)H_{B-R}(j,k)V(j,k)|^2+1\right\}\left(\frac{P_M}{N}\right)^{-1}\end{array}\right]}. \tag{18}$$

In Eq. (18), the equality holds if and only if

$$\begin{array}{l} \dfrac{V(0,k)}{G(0)H^*_{B-R}(0,k)H^*_{M-R}(0,k)} \\ = \ldots = \dfrac{V(j,k)}{G(j)H^*_{B-R}(j,k)H^*_{M-R}(j,k)} = \ldots = P(k) \end{array}, \tag{19}$$

where $P(k)$ the power allocation factor. Substituting Eq. (19) to Eq. (17) gives

$$\begin{array}{ll} \text{minimize } e_u = \sum_{k=0}^{N_c-1} \dfrac{\left\{B_u(k)P^2(k)+1\right\}\left(\frac{P_M}{N}\right)^{-1}}{A^2(k)P^2(k)+\left\{B_u(k)P^2(k)+1\right\}\left(\frac{P_M}{N}\right)^{-1}}, & \\ \text{s.t.} \quad \sum_{k=0}^{N_c-1}A(k)P^2(k)-N_c=0, & \\ \qquad P^2(k)\geq 0,\, k=0,\ldots,N_c-1 & \end{array} \tag{20}$$

where

$$\begin{cases} A(k) = \sum_{j=0}^{J-1}|G(j)H_{M-R}(j,k)H_{B-R}(j,k)|^2 \\ B_u(k) = \sum_{j=0}^{J-1}|G(j)H_{M-R}(j,k)H_{B-R}(j,k)|^2|G(j)H_{B-R}(j,k)|^2 \end{cases}. \tag{21}$$

The optimization problem of Eq. (20) can be solved using Karush-Kuhn-Tucker (KKT) conditions [15]. The Lagrangian function F is defined as

$$F = \left[\begin{array}{l} \sum_{k=0}^{N_c-1} \dfrac{\left\{B_u(k)P^2(k)+1\right\}\left(\frac{P_M}{N}\right)^{-1}}{A^2(k)P^2(k)+\left\{B_u(k)P^2(k)+1\right\}\left(\frac{P_M}{N}\right)^{-1}} \\ +\lambda_u\left\{\sum_{k=0}^{N_c-1}A(k)P^2(k)-N_c\right\}-\sum_{k=0}^{N_c-1}\tau(k)P^2(k) \end{array}\right], \tag{22}$$

where λ_u and $\{\tau(k):k=0,\ldots,N_c-1\}$ are the Lagrangian multipliers, respectively. The optimal power allocation factor $P^2(k)$ must satisfy the KKT condition as

$$\frac{\partial F}{\partial P^2(k)} = 0, \tag{23}$$

$$\sum_{k=0}^{N_c-1} A(k)P^2(k) - N_c = 0, \tag{24}$$

$$\lambda_u > 0, \tag{25}$$
$$P^2(k) \geq 0, \tag{26}$$
$$\tau(k) \geq 0, \tag{27}$$

and

$$-\tau(k)P^2(k) = 0. \tag{28}$$

When $\tau(k) = 0$, $P^2(k)$ is obtained from Eqs. (23) and (26) as

$$P^2(k) = \frac{1}{A(k)} \frac{\sqrt{\frac{A(k)}{\lambda_u}\left(\frac{P_M}{N}\right)^{-1}} - \left(\frac{P_M}{N}\right)^{-1}}{A(k) + \left(\frac{B_u(k)}{A(k)}\right)\left(\frac{P_M}{N}\right)^{-1}} > 0. \tag{29}$$

On the other hand, when $\tau(k) > 0$, $P^2(k)$ is obtained from Eqs. (26) and (28) as

$$P^2(k) = 0. \tag{30}$$

Therefore, $P^2(k)$ is given as

$$P^2(k) = \max\left[\frac{1}{A(k)} \frac{\sqrt{\frac{A(k)}{\lambda_u}\left(\frac{P_M}{N}\right)^{-1}} - \left(\frac{P_M}{N}\right)^{-1}}{A(k) + \left(\frac{B_u(k)}{A(k)}\right)\left(\frac{P_M}{N}\right)^{-1}}, 0\right]. \tag{31}$$

λ_u is chosen so as to satisfy Eq. (24).

Finally, the transmit FDE weight $V(j,k)$ is given from Eqs. (19) and (31) as

$$V(j,k) = \frac{G(j)H^*_{M-R}(j,k)H^*_{B-R}(j,k)}{\sqrt{A(k)}} \cdot \sqrt{\max\left[\frac{\sqrt{\frac{A(k)}{\lambda_u}\left(\frac{P_M}{N}\right)^{-1}} - \left(\frac{P_M}{N}\right)^{-1}}{A(k) + \left(\frac{B_u(k)}{A(k)}\right)\left(\frac{P_M}{N}\right)^{-1}}, 0\right]}. \tag{32}$$

Substituting Eq. (32) to Eq. (15), the receive FDE weight $W_B(k)$ is obtained.

3.2 Downlink Transmit and Receive FDE Weights

The optimization problem for obtaining the downlink transmit FDE weight is expressed as

$$\begin{aligned} &\text{minimize} \quad e_d \\ &\text{s.t.} \quad \sum_{k=0}^{N_c-1}\sum_{j=0}^{J-1}|V(j,k)|^2 - N_c = 0, \\ &\qquad |V(j,k)|^2 \geq 0, j = 0, \ldots, J-1, k = 0, \ldots, N_c - 1 \end{aligned} . \tag{33}$$

Similar to the case of uplink, we obtain the downlink transmit and receive FDE weights which minimizes the downlink MSE as

$$V(j,k) = \frac{G(j)H^*_{M-R}(j,k)H^*_{B-R}(j,k)}{\sqrt{A(k)}} \cdot \sqrt{\max\left[\frac{\sqrt{\frac{A(k)}{\lambda_d}\left(\frac{P_B}{N}\right)^{-1}} - \left(\frac{P_B}{N}\right)^{-1}}{A(k) + \left(\frac{B_d(k)}{A(k)}\right)\left(\frac{P_B}{N}\right)^{-1}}, 0\right]}, \tag{34}$$

where

$$B_d(k) = \sum_{j=0}^{J-1}|G(j)H_{M-R}(j,k)H_{B-R}(j,k)|^2|G(j)H_{M-R}(j,k)|^2 . \tag{35}$$

and λ_d is chosen so as to satisfy Eq. (6). Substituting Eq. (35) to Eq. (15), the receive FDE weight $W_M(k)$ is obtained.

4. Computer Simulation

The simulation model is illustrated in Fig. 4. $I = 6$ RSs are located along a circle with radius $r_{B-R} = 0.5$. The MT location is randomly generated in the cell. RS which has the largest short-term average SNR of MT-RS link is selected as

$$R = \underset{R' \in (0,1,\ldots,I-1)}{\operatorname{argmax}} \left[\frac{P_R}{N} r_{M-R'}^{-\alpha} 10^{-\frac{\eta_{M-R'}}{10}}\right]. \tag{36}$$

The propagation path loss exponent α is assumed to be $\alpha = 3.5$. The shadowing loss between MT and RS is assumed to be characterized by log-normal distribution having the standard deviation $\sigma = 7.0$ dB. The shadowing loss correlation $\rho_{R-R'}$ between Rth RS-MT link and R'th RS-MT link is considered. $\rho_{R-R'}$ is assumed to be given as [16]

$$\rho_{R-R'} = \xi \cos\theta_{R-R'} + \zeta, \tag{37}$$

where ξ and ζ are the setting parameters $\xi \geq 0$, $\zeta \geq 0$, $\xi + \zeta \leq 1$. ξ and ζ are set to $\xi = \zeta = 0.5$ in the computer simulation. On the other hand, BS-RS link is fixed and hence, the shadowing loss of BS-RS link can be controlled by choosing the RS location. The shot-term average

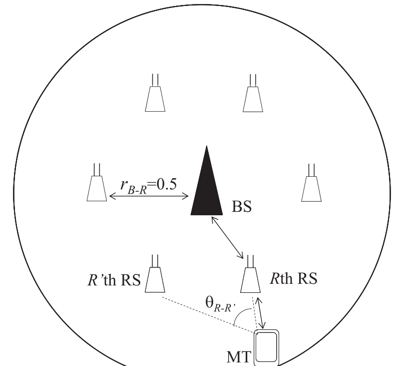

Fig. 4 Simulation model.

Table 1 Computer simulation condition.

Transmitter /receiver	Data modulation	QPSK, 16QAM
	FFT block size	$N_c = 128$
	CP length	$N_g = 16$
	Channel state information	Perfect
	Packet size	1536 bits
Channel	Fading type	Block Rayleigh fading
	Power delay profile	Symbol-spaced L-16path uniform
	Time delay	$\tau_l = l, l = 0, \ldots, L-1$
	Path loss exponent	$\alpha = 3.5$
	Shadowing loss standard deviation	$\sigma = 7.0$(dB)

SNR Γ of BS-RS link can be represented as

$$\Gamma = 10\log_{10}\frac{P_R}{N}r_{B-R}^{-\alpha} + \Delta\,(\text{dB}), \tag{38}$$

where Δ is the setting parameter and is determined by RS location. In the computer simulation, RSs are assumed to be located so as to satisfy $\Delta = 0$ dB.

The simulation condition is summarized in Table 1. QPSK and 16QAM data modulations are considered. FFT block size N_c and CP length N_g are set as $N_c = 128$ and $N_g = 16$, respectively. One packet consists of 1536 bits. A frequency-selective block Rayleigh fading having symbol-spaced L=16-path uniform power delay profile is assumed. For fair comparison with direct transmission, we assume the total transmit power constraint given as

$$P_B + P_R + P_M = P_T, \tag{39}$$

where P_T is the normalized total transmit power. In the computer simulation, $P_M = P_B = P_T/2$ is assumed for direct communication. On the other hand, when using ANC transmission, the power allocation of $P_R = P_T/2$ and $P_B = P_M = P_T/4$ is assumed. Also assumed are the ideal channel/noise estimation, perfect block synchronization, and perfect system synchronizations.

In this paper, the throughput S (bps/Hz) is define as

$$S = \frac{1}{2}M(1 - PER)\frac{N_c}{N_c + N_g}, \tag{40}$$

where M is the the number of bits per symbol and PER is the packet error rate. We evaluate, by computer simulation, the cumulative distribution function (CDF) of the throughput and CDF x% value is defined as x% outage throughput.

4.1 Transmit and Receive FDE Weights

Figure 5 shows the magnitudes of the transmit FDE weight at RS, the receive FDE weights at BS and MT, and the equivalent channel gain $|H_{M-R}(j,k)H_{B-R}(j,k)|$ between BS and MT link for J=2-antenna RS and the total transmit power-to-noise power ratio $P_T/N = 15$ dB. It can be seen from Figs. 5(a) and (b) that the most of transmit power is allocated to the antenna having high equivalent channel gain

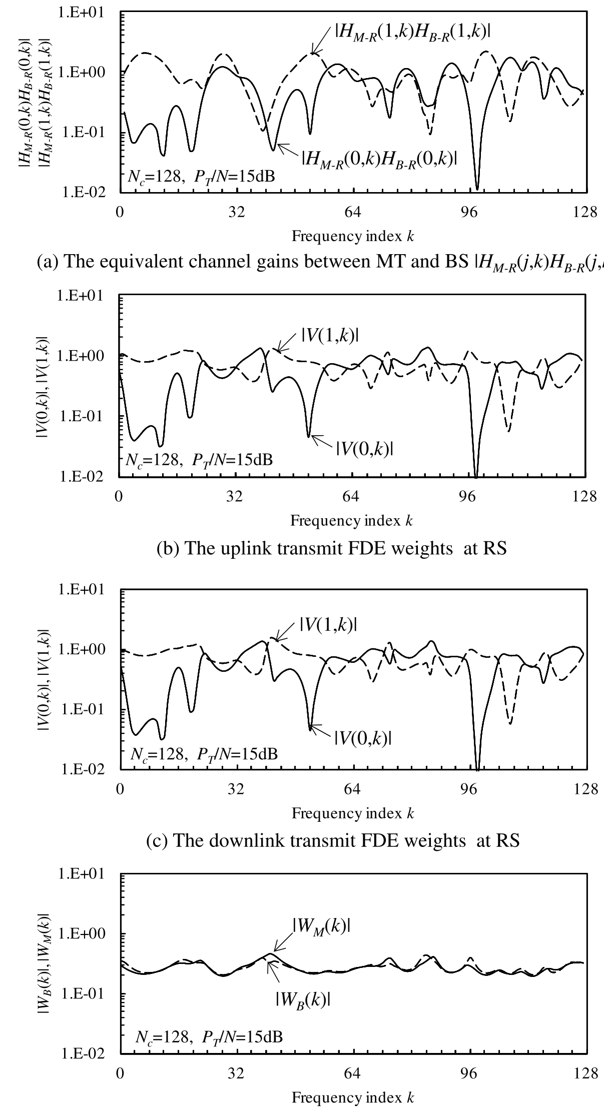

(a) The equivalent channel gains between MT and BS $|H_{M-R}(j,k)H_{B-R}(j,k)|$

(b) The uplink transmit FDE weights at RS

(c) The downlink transmit FDE weights at RS

(d) The receive FDE weights at BS and MT

Fig. 5 Transmit and receive FDE weights.

so as to maximize the spatial diversity gain. Furthermore, the transmit FDE acts as the zero-forcing equalization to remove the ISI. It is also seen from Figs. 5(a) and (d) that the variations of the receive FDE weight magnitude is smaller than the equivalent channel gain. This is because the residual ISI is sufficiently suppressed by diversity transmission using transmit FDE. It can also be seen from figures that the transmit FDE weight is almost the same for the uplink and downlink (see Figs. 5(b) and (c)). The reason for this is explained as follows. Since ANC relay utilizes a time division duplex (TDD), the uplink (MT→RS→BS) channel and the downlink (BS→RS→MT) channel are reciprocal. However, since the RS-BS channel and the RS-MT channel are different, the uplink SNR at BS is not the same as the downlink SNR at MT due to the existence of the noise transferred from RS. As a consequence, the common transmit FDE weight does not exist which minimizes both uplink and downlink mean square errors (MSEs) at the same time. However, the multi-antenna relay ($J > 1$) improves the received signal level at both BS and MT in the second time-slot and hence, the impact of transferred noise from RS to both BS and MT can be made sufficiently weak. If the uplink and downlink channels are reciprocal and the transferred noise from RS is negligible, the common transmit FDE weight exists which approximately minimizes both uplink and downlink MSEs at the same time.

4.2 Spatial and Frequency Diversity Gains Achievable by Joint Transmit/Receive FDE

Figure 6 plots the 10% outage throughput performance when using ANC transmission with the joint transmit/receive MMSE-FDE as a function of the normalized transmit power to noise power ratio P_T/N. For comparison, the performances when using the receive FDE only are also plotted in Fig. 6. It is shown from Fig. 6 that the joint transmit/receive FDE can always provides the throughput performance superior to the receive FDE only. Furthermore, the joint transmit/receive MMSE-FDE can improve the throughput performance as the number of RS antennas increases while the receive FDE only can hardly improve. This is because the joint transmit/receive MMSE-FDE can obtain the spatial diversity gain while the receive FDE only can hardly obtain it. When the number of RS antennas is $J = 4$, the joint transmit/receive MMSE-FDE can reduce by about 12 dB the transmit power for the given throughput $S = 1.6$ bps/Hz for both uplink and downlink.

Figure 7 compares the 10% outage throughput performances when using the joint transmit/receive FDE and the transmit FDE only. It is shown from Fig. 7 that the joint transmit/receive MMSE-FDE can improve the throughput performance compared to the transmit FDE only. This is because the joint transmit/receive MMSE-FDE can suppress ISI and obtain more frequency diversity gain than the transmit FDE only. The performance gap between the joint transmit/receive FDE and the transmit FDE only is large when high data modulation level is used. When $J = 1$, the joint transmit/receive FDE can reduce by about 4 dB the transmit power for the given throughput $S = 1.6$ bps/Hz compared to the transmit FDE only. This is because high data modulation

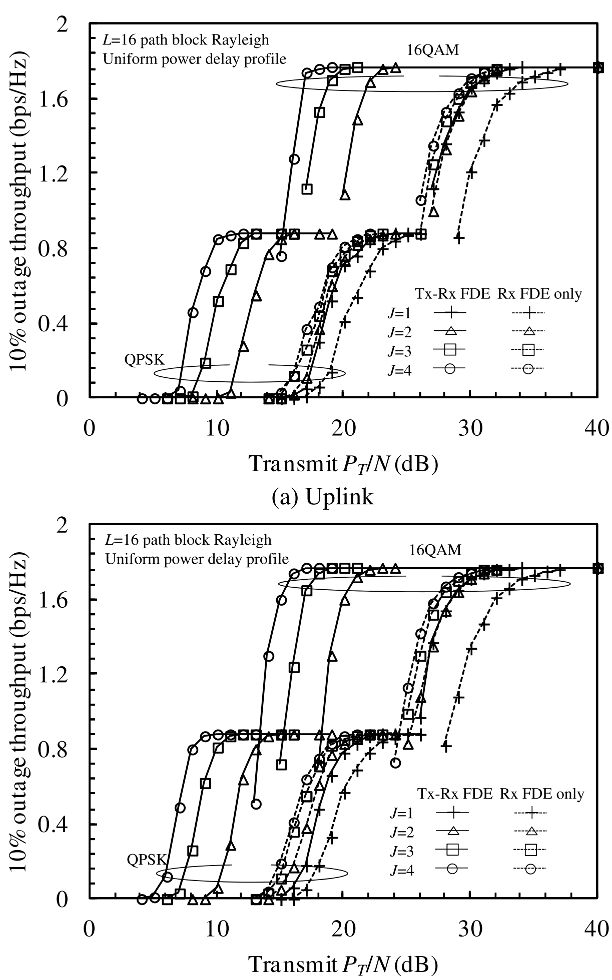

Fig. 6 Comparison of the receive FDE only.

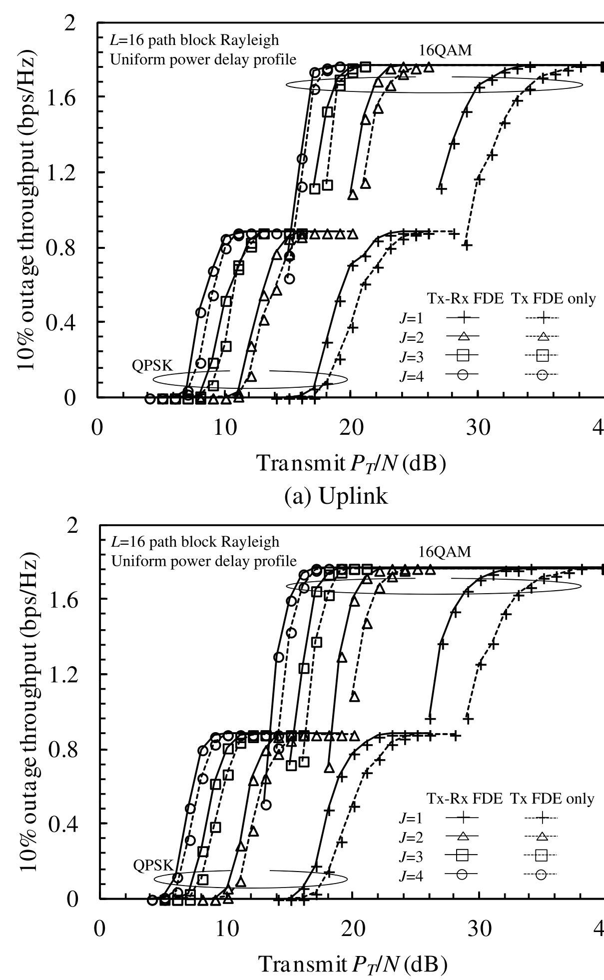

Fig. 7 Comparison of the transmit FDE only.

suffers from the residual ISI and the joint transmit/receive MMSE-FDE can further suppress the residual ISI compared to the transmit FDE only.

On the other hand, the performance gap between the joint transmit/receive FDE and the transmit FDE only reduce as the number of RS antennas increases. This is because the spatial diversity gain is larger than the frequency-diversity gain.

4.3 Comparison of Direct Transmission

In this subsection, we compare the performances when using multi-antenna ANC transmission and direct transmission and show multi-antenna ANC transmission can reduce the transmit power for the given throughput compared to direct transmission.

Figure 8 plots the 10% outage throughput performance when using the ANC transmission and direct transmission. It is shown from Fig. 8 that ANC transmission can reduce the required transmit power compared to direct transmission. Furthermore, multi-antenna ANC transmission can reduce the transmit power as the number of RS antennas increases. This is because multi-antenna ANC transmission with the joint transmit/receive MMSE-FDE can mitigate the impact of the propagation path loss and the shadowing loss with obtaining the spatial diversity gain. When the number of RS antennas is $J = 4$, multi-antenna ANC transmission can reduce the transmit power by about 23 dB for the given throughput $S = 1.6$ bps/Hz.

Figures 9 and 10 show the spatial distribution of 10% outage throughput in the cell. 16QAM data modulation is used and the normalized transmit power to noise power ratio P_T/N is set to $P_T/N = 20$ dB. When using direct transmission, the coverage which can achieve the given throughput is critically limited. When the given 10% outage throughput is 1.6 bps/Hz, the normalized radius r_{cover} of the coverage area

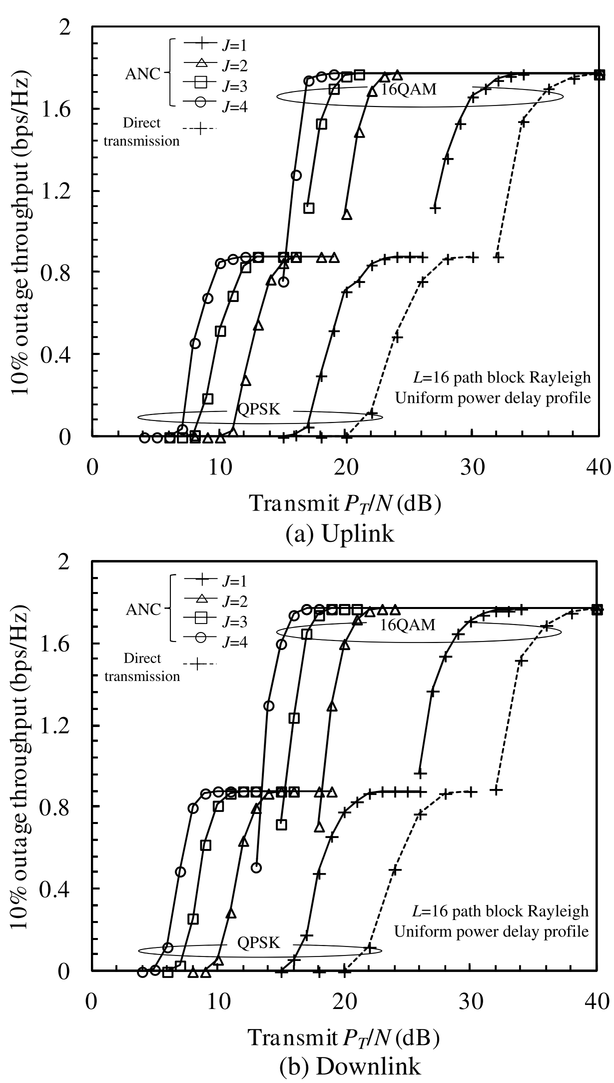

Fig. 8 10% outage throughput performance.

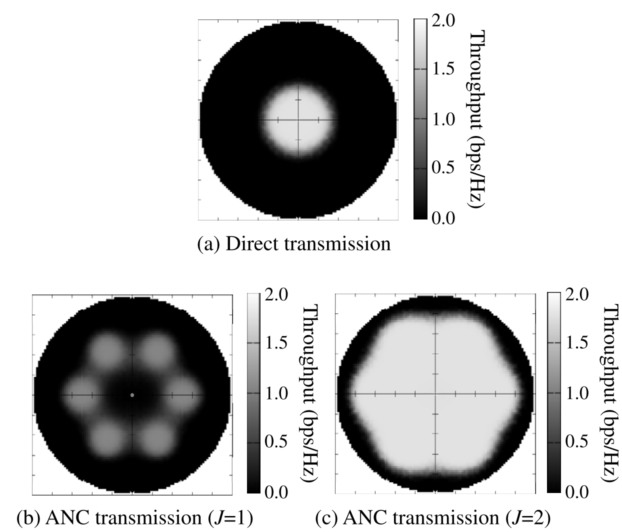

Fig. 9 10% outage uplink throughput distribution.

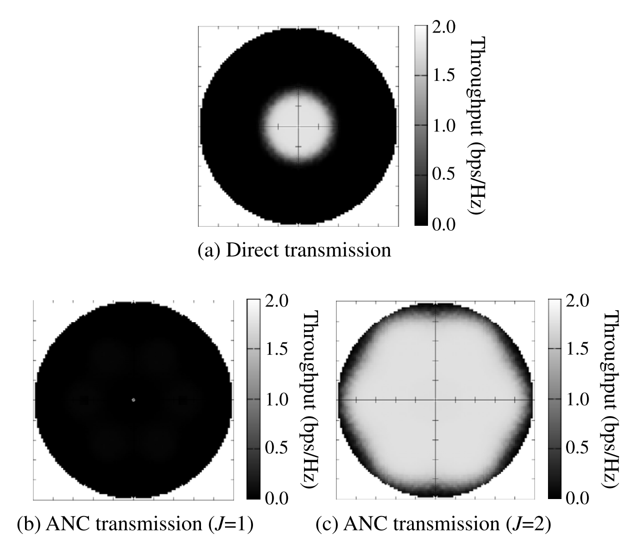

Fig. 10 10% outage downlink throughput distribution.

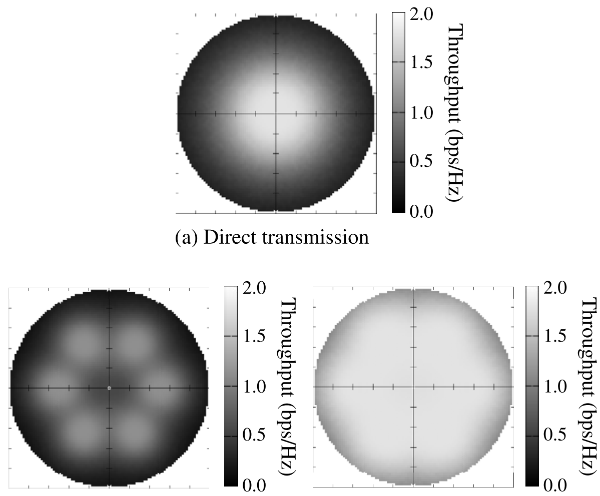

(a) Direct transmission

(b) ANC transmission (J=1) (c) ANC transmission (J=2)

Fig. 11 Average uplink throughput distribution.

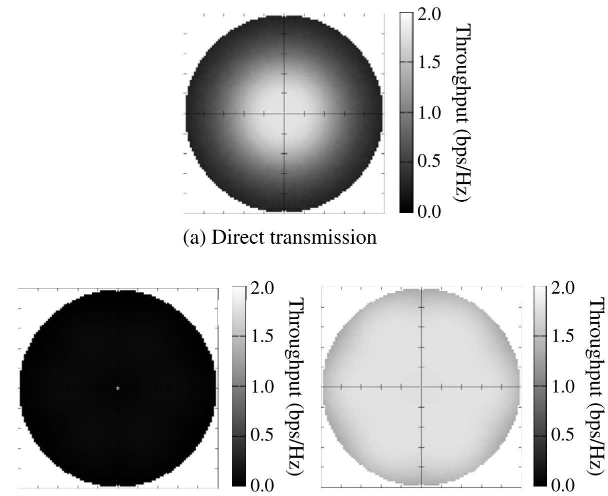

(a) Direct transmission

(b) ANC transmission (J=1) (c) ANC transmission (J=2)

Fig. 12 Average downlink throughput distribution.

limits r_{cover} = 0.3 when using direct transmission. This is because the received power drops by the negative impact of the propagation path loss and the shadowing loss when MT is located near the cell edge. It is also shown from Fig. 10 that single-antenna ANC relay ($J = 1$) can hardly extend the coverage area for downlink. The reason for this is explained as follows. In ANC relay, BS-MT direct link is not exploited as the cooperative relay since BS and MT simultaneously transmit signal in the first time-slot. Therefore, single-antenna ANC relay can obtain no spatial diversity gain, and hence, it suffers from the noise enhancement at RS. Therefore, single-antenna ANC relay can hardly extend the coverage area. On the other hand, multi-antenna ANC relay with the joint transmit/receive FDE can obtain the spatial diversity gain, and hence, it can significantly extend the coverage area compared to direct transmission. Multi-antenna ANC transmission with $J = 2$ can extend the normalized radius of coverage area to $r_{cover} = 0.8$ ($r_{cover} = 0.9$) for uplink (downlink). It is seen from Figs. 9 and 10 that the performance difference between uplink and downlink in multi-antenna ANC relay ($J = 2$) is smaller than that in single-antenna ANC relay ($J = 1$). This is because multi-antenna ANC relay ($J > 1$) improves the received signal level at both BS and MT and can make the impact of transferred noise from RS to both BS and MT sufficiently weak.

Figures 11 and 12 show the spatial distribution of the average throughput in the cell. 16QAM data modulation is used and the normalized transmit power to noise power ratio P_T/N is set to $P_T/N = 20$ dB. It is shown Figs. 11 and 12 that multi-antenna ANC transmission provides higher average throughput than direct transmission all over the cell. When MT is located at the cell edge, multi-antenna ANC transmission with $J = 2$ can provide 6 times (5 times) higher average downlink (uplink) throughput than direct transmission. This is because multi-antenna ANC transmission can achieve the same maximum throughput as direct transmission while mitigating the impact of the propagation path loss and the shadowing loss.

5. Conclusion

In this paper, we proposed a joint transmit/receive MMSE-FDE for ANC bi-directional relay communication using a multi-antenna relay. The proposed scheme performs transmit FDE at RS and receive FDE at BS and MT. The transmit/receive FDE weight is derived so as to minimize the end-to-end MSE of uplink and downlink. It was shown by the computer simulation that the joint transmit/receive FDE can improve the throughput performance compared to either the transmit FDE only or the receive FDE only. It was also shown by the computer simulation that multi-antenna SC ANC relay with joint transmit/receive FDE can significantly reduce the transmit power for the given throughput and can extend the coverage area compared to direct transmission.

In this paper, we discussed to what extent the proposed joint transmit/receive FDE improves the throughput performance compared to conventional transmission schemes (i.e., direct transmission and ANC single-antenna relay). The performance comparison to physical-layer network coding (PNC) [17] is an interesting future study.

References

[1] J.G. Laneman, D.N.C. Tse, and G.W. Wornell, "Cooperative diversity in wireless networks: Efficient protocols and outage behavior," IEEE Trans. Inf. Theory, vol.50, no.12, pp.3062–3080, Dec. 2004.

[2] S. Katti, H. Pahul, W. Hu, D. Katabi, M. Medard, and J. Crowcroft, "XORs in the air: Practical wireless network coding," IEEE/ACM Trans. Netw., vol.16, no.2, pp.497–510, June 2008.

[3] S. Katti, S. Gollakota, and D. Katabi, "Embracing wireless interference: Analog network coding," Proc. ACM SIGCOMM, pp.397–408, Aug. 2007.

[4] H. Gacanin and F. Adachi, "Broadband analog network coding," IEEE Trans. Wireless Commun., vol.9, no.5, pp.1577–1783, May 2010.

[5] S. Zhang, S.C. Liew, and P.P. Lam, "Hot topic: Physical-layer network coding," Proc. ACM 12th MobiCom 2006, pp.358–365, Sept.

2006.
[6] J.G. Proakis, Digital Communications, 4th ed., McGraw-Hill, 2001.
[7] R. Prasad, OFDM for wireless communications systems, Artech House, 2004.
[8] H. Han and J.H. Lee, "An overview of peak-to-average power ratio reduction techniques for multicarrier transmission," IEEE Wireless Commun. Mag., vol.12, no.2, pp.56–65, April 2005.
[9] D. Falconer, S.L. Ariyavistakul, A. Benyamin-Seeyar, and B. Eidson, "Frequency domain equalization for single-carrier broadband wireless systems," IEEE Commun. Mag., vol.40, pp.58–66, April 2002.
[10] F. Adachi, H. Tomeba, and K. Takeda, "Introduction of frequency-domain signal processing to broadband single-carrier transmissions in a wireless channel," IEICE Trans. Commun., vol.E92-B, no.9, pp.2789–2808, Sept. 2009.
[11] K. Takeda and F. Adachi, "Joint transmit/receive one-tap minimum mean square error frequency-domain equalization for broadband multicode direct-sequence code division multiple access," IEEE Trans. Signal Process., vol.58, no.10, pp.5463–5468, Oct. 2010.
[12] Y. Liang, A. Ikhlef, W. Gerstacker, and R. Schober, "Filter-and-forward beamforming for multiple multi-antenna relays," Proc. CHINACOM, 2010 5th International ICST Conference, pp.1–8, Aug. 2010.
[13] R. Zhang, C.C. Chai, Y.C. Liang, and S. Cui, "On capacity region of two-way multi-antenna relay channel with analogue network coding," Proc. IEEE Intern. Conf. on Commun., pp.1–5, June 2009.
[14] R. Zhang, Y.C. Liang, C.C. Chai, and S. Cui, "Optimal beamforming for two-way multi-antenna relay channel with analogue network coding," IEEE J. Sel. Areas Commun., vol.27, no.5, pp.699–712, June 2009.
[15] S. Boyd and L. Vandenberghe, Convex optimization, Cambridge University Press, 2003.
[16] S.S. Szyszkowicz, H. Yanikomeroglu, and J.S. Thompson, "On the feasibility of wireless shadowing correlation models," IEEE Trans. Veh. Technol., vol.59, no.9, pp.4222–4236, Nov. 2010.
[17] H.H. Chung, S.H. Kuo, and M.C. Lin, "A physical-layer network coding scheme based on linear MIMO detection," Proc. IEEE 75th Vehicular Tech. Conf. (VTC), pp.1–5, May 2013.
[18] H. Miyazaki, M. Nakada, T. Obara, and F. Adachi, "Joint transmit/receive MMSE-FDE for MIMO analog network coding in single-carrier bi-directional relay communications," Proc. IEEE 71st Vehicular Tech. Conf. (VTC), pp.1–5, Sept. 2012.

Hiroyuki Miyazaki received his B.S. degree in Information and Intelligent Systems from Tohoku University, Sendai Japan, in 2011. Currently he is a graduate student at the Department of Communications Engineering, Graduate School of Engineering, Tohoku University. His research interests include cooperative amplify-and-forward relay and network coding systems.

Tatsunori Obara received his B.S. degree in Electrical, Information and Physics Engineering in 2008 and M.S. degree in communications engineering, in 2010, respectively, from Tohoku University, Sendai Japan. Currently he is a Japan Society for the Promotion of Science (JSPS) research fellow, studying toward his PhD degree at the Department of Electrical and Communications Engineering, Graduate School of Engineering, Tohoku University. His research interests include channel equalization techniques for mobile communication systems.

Fumiyuki Adachi received the B.S. and Dr. Eng. degrees in electrical engineering from Tohoku University, Sendai, Japan, in 1973 and 1984, respectively. In April 1973, he joined the Electrical Communications Laboratories of Nippon Telegraph & Telephone Corporation (now NTT) and conducted various types of research related to digital cellular mobile communications. From July 1992 to December 1999, he was with NTT Mobile Communications Network, Inc. (now NTT DoCoMo, Inc.), where he led a research group on wideband/broadband CDMA wireless access for IMT-2000 and beyond. Since January 2000, he has been with Tohoku University, Sendai, Japan, where he is a distinguished Professor of Communications Engineering at the Graduate School of Engineering. His research interest is in the areas of wireless signal processing and networking including broadband wireless access, equalization, transmit/receive antenna diversity, MIMO, adaptive transmission, channel coding, etc. He was a program leader of the 5-year Global COE Program "Center of Education and Research for Information Electronics Systems" (2007–2011), awarded by the Ministry of Education, Culture, Sports, Science and Technology of Japan. From October 1984 to September 1985, he was a United Kingdom SERC Visiting Research Fellow in the Department of Electrical Engineering and Electronics at Liverpool University. He is an IEICE Fellow and was a co-recipient of the IEICE Transactions best paper of the year award 1996, 1998, and 2009 and also a recipient of Achievement award 2003. He is an IEEE Fellow and a VTS Distinguished Lecturer for 2011 to 2013. He was a co-recipient of the IEEE Vehicular Technology Transactions best paper of the year award 1980 and again 1990 and also a recipient of Avant Garde award 2000. He was a recipient of Thomson Scientific Research Front Award 2004, Ericsson Telecommunications Award 2008, Telecom System Technology Award 2009, and Prime Minister Invention Prize 2010.